American Journal of Materials Synthesis and Processing
2018; 3(3): 47-55
http://www.sciencepublishinggroup.com/j/ajmsp
doi: 10.11648/j.ajmsp.20180303.12
ISSN: 2575-2154 (Print); ISSN: 2575-1530 (Online)

Separation of Surface Hardened Glass with Non-ablation Laser Technique

Zhongke Wang[1, *], Wei Liang Seow[2], Hongyu Zheng[1, 3, *], Cai Xue[2]

[1]Singapore Institute of Manufacturing Technology (SIMTech), Singapore

[2]Department of Material Science and Engineering, Nanyang Technological University (NTU), Singapore

[3]School of Mechanical Engineering, Shandong University of Technology, Zibo, China

E-mail addresses:

zkwang@simtech.a-star.edu.sg (Zhongke Wang), hyzheng@simtech.a-star.edu.sg (Hongyu Zheng)

[*]Corresponding author

To cite this article:

Zhongke Wang, Wei Liang Seow, Hongyu Zheng, Cai Xue. Separation of Surface Hardened Glass with Non-ablation Laser Technique. *American Journal of Materials Synthesis and Processing*. Vol. 3, No. 3, 2018, pp. 47-55. doi: 10.11648/j.ajmsp.20180303.12

Received: July 9, 2018; **Accepted**: September 28, 2018; **Published**: November 6, 2018

Abstract: The study investigated cutting of glass by non-laser ablation technique through non-linear absorption laser pulses induced optical breakdown, melting and plasma expansion throughout the glass thickness from bottom to top. Picosecond near-infrared laser pulses were used. The laser beam was focused with an objective lens with numerical aperture (NA) of 0.1 which produced a spot size of 19.6 μm in diameter. The study revealed that focus position is a key factor in determining glass well-separation. When the laser focus was placed at 500 μm below the top surface for a 700 μm thick ion exchanged Gorilla glass, namely more than half of the glass thickness, the glass could be well-separated into two pieces. At focus near the top surface, V-shaped ablation grooves were generated at the glass top surface without glass separation. At focus inside the glass and near to the bottom surface, internal scribing occurred at the bottom part of the glass. The glass could also be separated by scribing-caused cracking throughout the glass entire thickness. At the optimal focus ranges, well-separation of the glass was found to be at speeds of 0.5-6 mm/s and pulse frequency around 200 KHz with laser fuence of 0.87 J/cm^2. At low pulse frequencies such as below 100 KHz, glass top surface was ablated without glass separation. At higher pulse frequencies above 300 KHz, cracks were produced and the glass was separated into multiple pieces. Interestingly, at pulse frequency upto 500 KHz, both top surface ablation and bottom surface ablation occurred. Eventually, the glass was cracked into multiple pieces. Different pulse frequency produces different pulse energy. For example, 200 KHz generates a laser fluence of 0.87 J/cm^2 at the glass top surface, 100 KHz for 1.59 J/cm^2 and 300 KHz for 0.60 J/cm^2 etc. Furthermore, the glass was cracked at high speeds above 10 mm/s. The results indicate that there is an optimal time-dependent energy deposition, namely, laser energy deposition rate for glass well-separation. The calculation shows that the energy deposition rates were between 1.29×10^4 μw/μm^3 to 1.54×10^5 μw/μm^3.

Keywords: Glass Cutting, Laser Ablation, Surface Hardened Glass, Laser Cutting

1. Introduction

Surface strengthened glasses such as Corning Gorilla, Asahi Dragontrail, Schotts Xensation have been used primarily in portable consumer electronic devices to help protect from every-day wear and tear. Such glasses are under compressive stress at its surface and tensile stress at its middle. For the first generation of chemically surface-strengthened glass developed in the 1960s, the traditional techniques mechanical scribe and break, grinding and sawing were sufficient, but with the increasing stress levels of the new generations of glasses developed in the 2000s, they have become unviable. Once the scribing or sawing is deep enough to reach the tensile zone in the middle, crack tips are under tensile stress, causing rapid, spontaneous, and chaotic propagation of cracks in the tensile center layer, which results in the destruction of the entire part. New cutting methodologies are needed.

When looking at the laser glass cutting history, well-developed methods such as laser fusion cutting with CO_2

lasers [1], laser surface scribing followed with post force breaking [2], laser cleavage with coolant-assistance [3], laser internal scribing [4] and pulsed laser ablation [5]. For laser separation of chemically strengthened glass, it has been reported that initial flaw on the glass surface or on the glass edge followed with an elongated elliptical beam scanning and rapid cooling enables clean full separation of the strengthened glass sheets [6]. Other attractive methods involves such as ultrashort laser pulses ablation reported in 2013 [7] and in 2014 [8], laser filamentation cutting [9]. Laser filamentation cutting is through utilising an ultrashort picosecond (ps) laser operating in a burst mode for the generation of a self-focused laser beam inside the glass. To some degree, when filamentation cutting achieves curved cuts, since there is a zero kerf width, separation of the components can be a problem because the cut parts are effectively locked inside the hole they are cut from [10]. In this case, ultrashort pulsed laser ablation shows big advantages [11]. It has been further disclosed on how to improve the laser ablation efficiency [12].

This study explores other non-ablation laser ablation technique rather than filamentaion for separation of surface chemically hardened glass with ps laser. Special effort was placed on the influence of laser process parameters such as focus position inside glass, pulse frequency and scanning speed etc. during separation of the glass under a single of the ps laser beam.

2. Experiments

A ps laser (Time-Bandwidth DUETTO, Switzerland) was used to irradiate a 700 µm thick exchanged Gorilla glass substrate (Corning, USA) which was commercially available. Wavelength of the laser was 1064nm. Beam quality M2 of of the laser was <1.3. Pulse frequency of the laser was 50 KHz to 8.2 Mhz. Pulse duration of the laser was <12 ps. Nominal output power of the laser was 10 W to 15 W. A 0.1 NA objective lens was used to focus the laser beam, which produced a spot size of approximately 19.6 µm. After the focus lens, the laser power measured was to be 3.55 W at the lowest repetition rate of 50 KHz, which could produce a maximum laser fluence of 7.46 J/cm$^{2.}$ At higher frequency from 100 KHz to 1000 KHz, laser power was measured to be from 4.11 W to 5.01 W. The laser irradiation was through fix optics and sample was moved by x-y table. The glass substrate was translated with respect to a stationary laser beam at speeds ranging from 0.5 mm/s to 600 mm/s. The glass cutting was carried out at different focus position, pulse frequency and scanning speed.

3. Results and Discussion

3.1. Effect of Focus Position

3.1.1. Optimal Laser Focus for Cut Through of the Glass

Laser focus position here refers to the position at which the laser focus spot is placed relative to the glass top surface. Figure 1 shows the schematic of laser focus position inside the glass. Different cutting phenomena were observed when the laser focus was changed and placed at different positions in the glass thickness direction. When the laser focus was placed from 300 µm above to 400 µm below glass top surface, top surface ablation was observed. However, there was no glass separation occurred. When the laser focus was placed 500 µm to 600 µm below glass top surface, i.e. at 200 µm to 100 µm above glass bottom surface, no surface ablation was observed. However, the glass substrate could be well separated into two pieces. When the laser focus was placed near to the glass bottom surface, bottom ablation occurred but mainly internal scribing near to the glass bottom surface was obtained. The glass was separated too. The scribed length in glass thickness direction was more than half of the glass thickness from the glass bottom surface to the glass center. The top part of glass thickness was separated by cracking, as shown in figure 1. When the laser beam focus was placed outside and 100 µm below the bottom surface, both top and bottom surface ablation occurred. However, there was no glass separation. Clearly, there was an optimal focus position for glass substrate separation. The focal plan should be placed at a position around the two-thirds of the glass thickness.

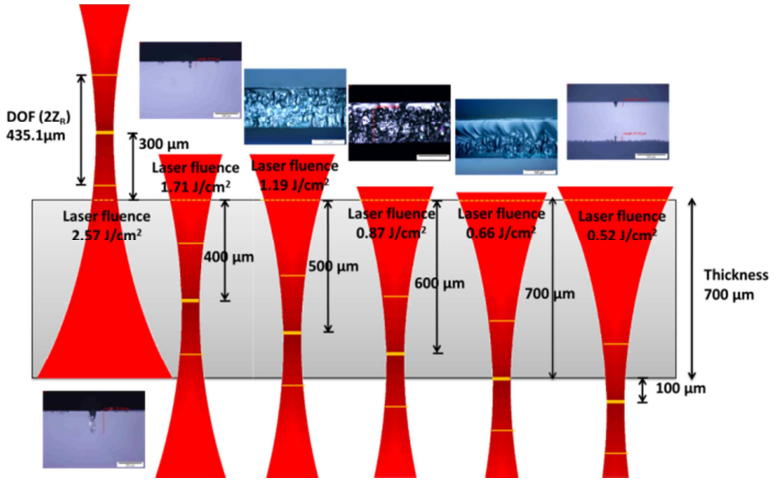

Figure 1. *Schematics of the position of the laser focus in the glass thickness direction. Optical images were from samples cut at pulse frequency of 200 KHz and laser scanning speed of 0.5 mm/s.*

Different focus position refers to the different spot size deposited at the glass top surface. Thus, different laser fluences were obtained at the glass top surface with changing of the laser focus. The values of the laser fluence can be obtained simply by dividing laser pulse energy by the laser spot area at the glass top surface, as seen in Figure 1.

The results have clearly revealed that focus position is an important parameter in determining whether the glass can be cut through. The optimal focus position for well-separation of the glass without cracking is the laser focus placed at 500 μm to 600 μm below the glass top surface. The laser fluence at the laser beam focus is 7.46 J/cm^2. The laser fluence at the glass top surface was 1.19 J/cm^2 and 0.87 J/cm^2 respectively at these two focus positions. When the laser focus was placed from 300 μm to 400 μm below the glass top surface, V-shaped ablation grooves were formed at the glass top surface. The width of the ablation grooves was found to correlate with the laser beam diameter at the glass top surface. The depth of the ablation grooves were related to the logarithmic dependence of the laser fluence. When the laser focus was placed near to the glass bottom surface and inside the glass, the laser fluence at the glass top surface is 0.66 J/cm^2. When the laser beam focus was placed outside and 100 μm below the glass bottom surface, top and bottom surface ablation occurred. The laser fluence at the glass top surface is 0.52 J/cm^2. It indicates that there are optimal laser fluences for the glass separation without breakage into multiple pieces under the laser beam irradiation. The study further identified that the optimal laser focus position inside glass remained constant when increasing the laser beam scanning speed.

3.1.2. Mechanism for Glass Separation

The laser beam used with 1064 nm wavelength is transparent to the glass. This allows the laser focus to be placed at different locations inside the glass. Figure 2 shows the sidewall image of the glass cut under the laser focus positioned at 500 μm to 600 μm below the glass top surface at 200 KHz pulse frequency and scanning speed of 0.5 mm/s. Glass optical breakdown, melting, small vertical voids resulted from plasma explosion and microcracks at the sidewalls can be observed and these phenomena of optical breakdown, melting, plasma explosion, etc. allow the glass to be well separated.

Due to the ultrashort ps pulse width, high laser intensity was achieved at the laser focus which resulted in plasma formation inside the glass by multi-photon absorption. Several phenomena have been disclosed which covers the inverse bremsstrahlung [13], the avalanche collision [14], the optical breakdown [15] and vertical void formation [16]. It has been summarized that the mechanism of optical breakdown involves all the multi-photon absorption, inverse Bremstrallung and avalanche collision [17]. Multi-photon absorption is the absorption of multiple photons causing the excitation of electron from valence band to conduction band producing free electrons. Inverse Bremsstrahlung refers to the free electrons absorbing or emitting photons while colliding (scattering) with a much heavier particle and gaining kinetic energy in the process. When the free electron acquires a kinetic energy higher than the ionization potential of the gas molecule/atom, the electron can collide with other atoms in the material to expel an extra electron from the molecule/atom resulting in two energy electrons. These two electrons then undergo inverse Bremsstrahlung again to kick out another two more electrons from other atoms. It has been revealed that this is called cascade or avalanche ionization which causes the growth of the electron density to form plasma [18]. In this case, melting and plasma explosion was caused by the plasma being heated up to high temperature by the laser beam due to the slow scanning speed used. After the heated plasma relaxed the thermal energy to the lattice, the glass material can be heated to above the melting point or even above the boiling point resulting in melting and plasma explosion inside the glass. Plasma explosion can be described by molten material exploding out of the heated zone which manifests itself in the form of small vertical voids and cracks at the sidewalls [15], as shown in figure 2. Eventually, plasma explosion, optical breakdown, small vertical voids and melting, etc. inside the glass throughout entire thickness of the glass caused the glass well separated without broken into multiple pieces at the optimal focus with laser fluence at the glass top surface was 0.87-1.19 J/cm2 and 7.46 J/cm2 at the focus inside the glass.

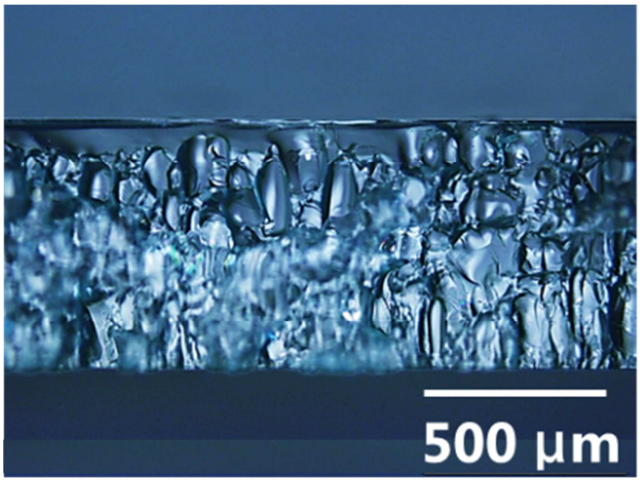

Figure 2. *Optical image of the side wall of the glass cut at 0.5 mm/s scanning speed.*

3.2. Effect of Pulse Frequency

Pulse frequency is the number of pulses emitted by the laser in one second. When pulse frequency increases, pulse energy drops simultaneously for the ps laser used in our experiments, as shown in figure 3. At the optimal focus position for well-separation of the glass namely the laser focus placed at 500-600 μm below the glass top surface, laser irradiation with various laser pulse frequences has been carried out in order to determine the effect of pulse frequency.

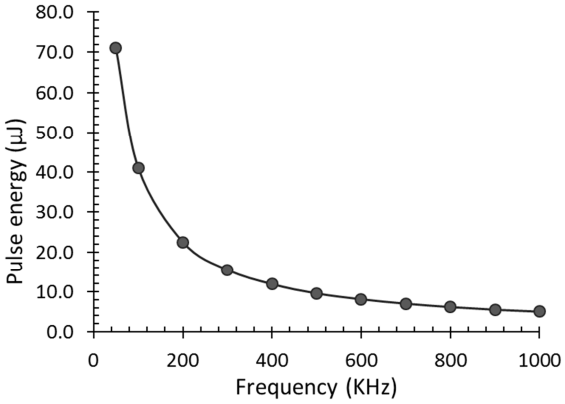

Figure 3. *Inverse relationship between pulse energy and pulse frequency.*

At 50 KHz and 100 KHz pulse frequency, the high pulse energy of 71 μJ and 41.1 μJ led to high laser fluence of 3.77 J/cm2 and 2.18 J/cm^2 at the top surface respectively. As a result, mainly top surface ablation occurred as shown in figure 4. Despite laser focus being placed near the glass bottom surface, the high laser fluence at the top surface due to the low pulse frequency led to mainly top surface ablation. Only a slight crack occurs at the bottom surface which indicates majority of the pulse energy is absorbed at the glass top surface.

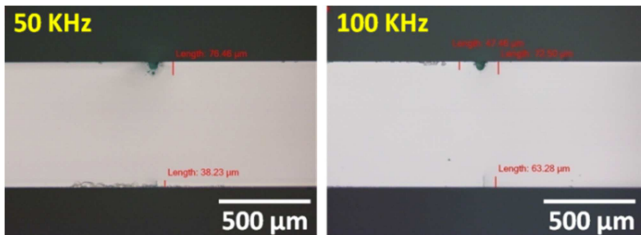

Figure 4. *Optical images of ablation grooves with slight bottom surface crack at pulse frequency of 50 KHz and 100 KHz.*

At 200 KHz pulse frequency, the pulse energy was lowered to 22.5 μJ which produced a laser fluence of 1.19 J/cm^2 at the top surface and resulted in well-separated as shown in figure 2. The lower laser fluence at the glass top surface could result in less top surface ablation. Without top surface ablation, more portion of the pulse energy can go inside the glass. At discussed above, optimal focus position and fluences, the glass can be well separated without cracking into multiple pieces.

At 300 KHz and 400 KHz, the pulse energy is lowered to 15.5 μJ and 11.9 μJ and the laser fluence at the top surface was lowered to 0.82 J/cm^2 and 0.63 J/cm^2 respectively. This resulted in no ablation observed at the top and bottom surfaces and only internal cracks generated inside the glass. No ablation was observed which indicates that the laser fluence at the glass top and bottom surface were lower than the ablation threshold. As the laser fluence at the beam focus was lowered to 5.13 J/cm^2 and 3.94 J/cm^2 respectively, these laser fluences are insufficient to cause melting inside the glass. Instead, the heat is dissipated to form internal cracks inside the glass as shown in figure 5. Such a result is agreed with the report by Karlsson [19], the laser-induced phenomena generated internal stresses inside the glass which are amplified by the intrinsic inner tensile stress of the ion-exchanged glass and causes cracking of the glass into multiple pieces.

At 500 KHz, the reduced laser fluence at the top surface of 0.51 J/cm^2 resulted in top surface ablation

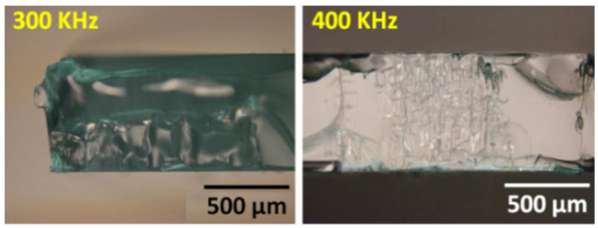

Figure 5. *Optical images of glass sidewall cut at pulse frequency of 300 KHz and 400 KHz.*

Melting and bottom surface ablation as shown in figure 6. In this case, despite the pulse energy drop to 9.56 μJ, reducing the laser fluence at glass top surface and at the laser focus, higher pulse number deposited due to the higher pulse frequency could also resulted in top and bottom surface ablation and melting inside the glass which is not observed at 300 KHz and 400 KHz. Steen reported that top and bottom surface ablation may be caused by more pulses deposited leading to rise in glass surface temperature and increased absorption of laser beam energy [20]. Machado et al reported that higher pulse number deposited can also create more defects at glass surfaces which could lower ablation threshold [21]. Thus, due to the higher pulse frequency, more pulses deposited may heat up the plasma generated inside the glass to high temperature to cause melting inside the glass.

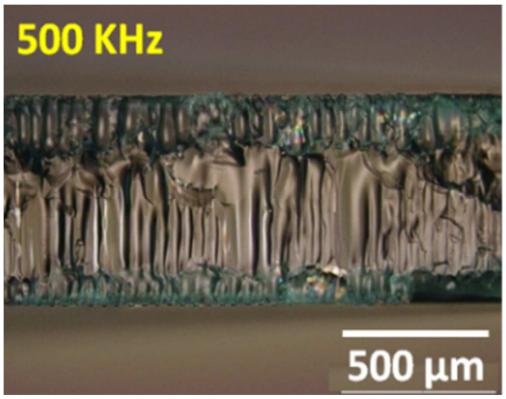

Figure 6. *Optical image of sidewall of the glass cut at pulse frequency of 500 KHz.*

At 600 KHz, the laser fluence at the glass top surface was lowered to 0.43 J/cm^2 which resulted in elongated voids observed extending from laser focus to slightly below the top surface, slight bottom surface ablation with no signs of top surface ablation as shown in figure 7. This indicates that the laser fluence of 0.43 J/cm^2 at the glass top surface was lower than the ablation threshold while the laser fluence at the bottom surface of 1.46 J/cm^2 was above the ablation threshold. The vertical voids generated could be due to optical

breakdown. This indicates that laser intensity was above the optical breakdown threshold. The laser intensity at focus was obtained by dividing pulse energy by the laser spot size at focus and laser pulse width. The vertical voids formed had a smaller width at the laser focus due to the smaller diameter at the laser beam focus. The width of the void was wider away from the laser focus near the glass top surface due to the larger beam diameter away from the laser focus as shown in figure 7.

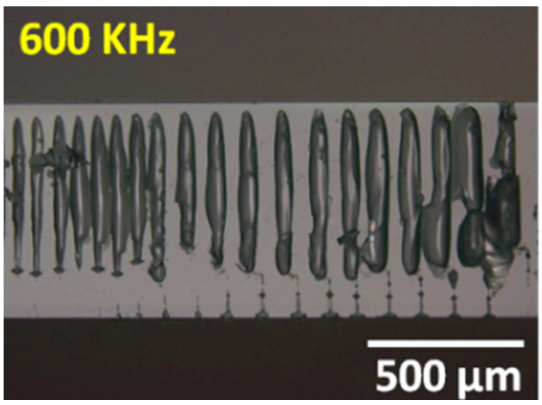

Figure 7. *Optical image of sidewall of the glass cut at pulse frequency of 600 KHz.*

For 700 KHz to 1000 KHz, the laser fluence at glass top surface was reduced from 0.37 J/cm2 to 0.27 J/cm^2 which resulted in cracks and modified regions observed at the glass sidewall as shown in figure 8. No significant ablation was observed which indicates that the laser fluence at the glass top and bottom surface were lower than the ablation threshold. This indicates that the laser intensity at focus of 1.38×1011 W/cm^2 to 1.93×1011 W/cm^2 for these pulse frequencies were close to the optical breakdown threshold intensity to generate these modified regions which may be smooth refractive index changes within the glass. The results are agreed with the discussion from Eaton et al that the modified regions observed at the sidewall of the cut glass could be due to smooth refractive index changes [22].

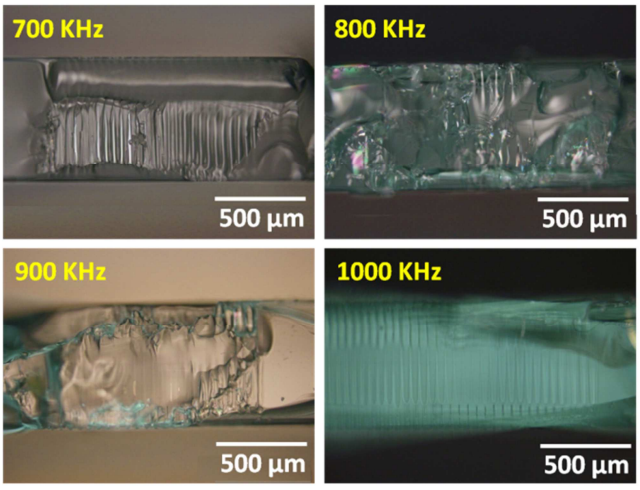

Figure 8. *Optical images of the sidewall of the glass cut at pulse frequency of 700 KHz, 800 KHz, 900 KHz and 1000 KHz*

3.3. Effect of Laser Scanning Speed

Laser scanning speed refers that how fast the laser spot is relatively moved along a workpiece to be machined. The scanning speed together with pulse frequency determines the amount of total laser energy deposited into the glass focal volume. The time dependent energy amount can be describe using laser energy deposition rate.

Laser energy deposition rate can be calculated as the amount of laser energy deposited per unit glass focal volume in one second as given in below equation:

$$R_d = \frac{E_p}{T} \times N_{pulse} \times \frac{1}{V_f}$$

Where
Rd: Laser energy deposition rate [w/m3]
Ep: Laser pulse energy [J]
Npulse: Pulse number
T: Pulse period [s]
Vf: Glass focal volume

The glass focal volume, Vf, as shown in figure 9, is defined by the laser interaction volume within the glass upon laser irradiation which can be calculated by:

$$V_f = \int_a^b \pi . w(z)^2 dz = \left[\pi {w_0}^2 z + \frac{\lambda^2 (M^2)^2}{\pi {w_0}^2} \left(\frac{z^3}{3}\right) \right]_a^b$$

Where
W(z): Beam radius at z distance from the beam focus where the intensity drops to 1/e2 (≈ 13.5%) of the maximum value
λ: Laser wavelength
M2: Beam quality factor
W0: Laser focus spot diameter
a: z-value of focus position at glass bottom surface
b: z-value of focus position at glass top surface
z: Distance from the beam focus

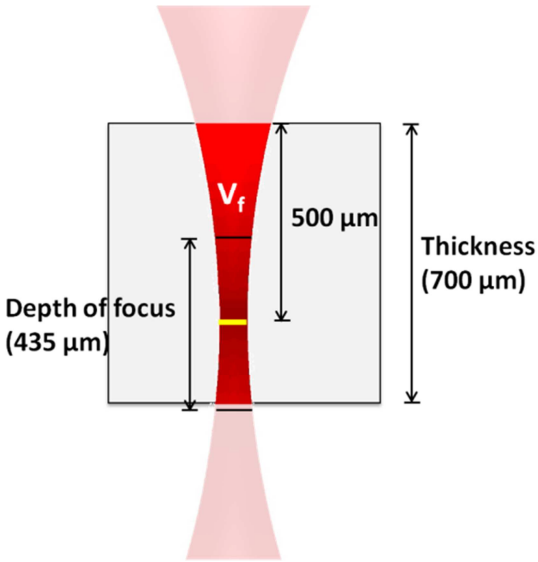

Figure 9. *Schematic of glass focal volume within the glass thickness.*

Figure 10 shows the plot of laser deposition rate versus scanning speed for a pulse frequency of 200 KHz. The focus was placed at 500 μm below the glass top surface. Given a fixed laser focus position and pulse frequency, the laser focal volume within the glass and the pulse energy were fixed respectively. Hence, the laser deposition rate depended only on the pulse number deposited into the glass. When laser scanning speed was increased, lesser laser pulses were deposited into the focal volume which led to a decrease in laser energy deposition rate.

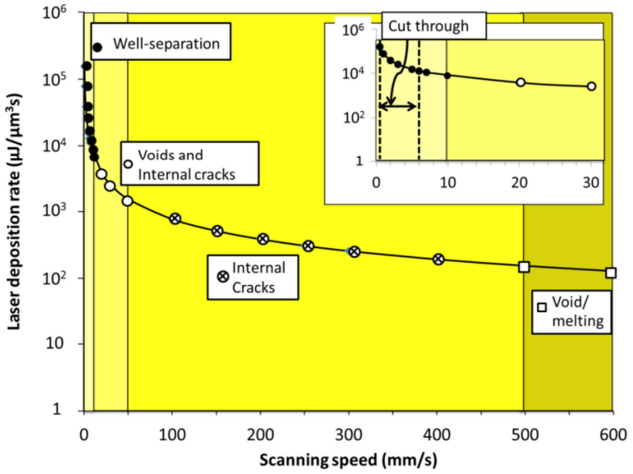

Figure 10. *Plot of laser deposition rate versus laser scanning speed.*

In figure 10, it is also shown that as scanning speed increases, different cutting phenomena occurred. From 0.5 mm/s to 6 mm/s, the glass could be well-separated without cracking. Above 10 mm/s, the drop in laser deposition rate and total energy deposited into the focal volume leads to cracking of the glass. At low scanning speed from 0.5 mm/s to 10 mm/s scanning speed, melting and plasma explosion occurred inside the glass. At 20 mm/s to 50 mm/s scanning speed, cracks and optical breakdown near the bottom of the glass thickness occurred. At 100 mm/s to 400 mm/s scanning speed, only cracks inside the glass were observed. At 500 mm/s and 600 mm/s scanning speed, voids occurred near the glass top surface with melting tracks extending from the bottom of the void.

From 0.5 mm/s to 6 mm/s scanning speed, the high laser energy deposition rate ranging from 1.79×105 μw/μm^3 to 1.49×104 μw/μm^3 allows crack-free separation of the glass. Above 10 mm/s speed, the drop in laser deposition rate and total energy deposited into the focal volume led to cracking of the glass. Due to the drop in laser deposition rate, the glass could not be cut through completely. Hence, the laser induced-internal stress which was amplified by the intrinsic inner tensile stress of the ion-exchanged glass caused the glass to crack into multiple pieces.

For 0.5 mm/s scanning speed, the high laser deposition rate of 1.79×105 μw/μm^3. leads to on top and bottom surfaces slight scribing, melting as well as plasma explosion in the form of voids occurring inside the glass as shown in figure 11. The high laser deposition rate resulted in top surface ablation due to heating of the glass top surface which increased laser beam absorption and the earlier pulses may generate defects at the glass top surface which lowered the ablation threshold. In addition, the focus placed near to the bottom surface also resulted in sufficient laser fluence for bottom surface ablation. The plasma explosion and melting occurring inside the glass could be due to the heating up of the plasma inside the glass to high temperatures at a high laser deposition rate. As Steen et al investigated when the thermal energy of the heated plasma was released into the lattice, this causes the glass to be heated up above its melting temperature or even above the boiling point to drive plasma explosion inside the glass [20]. The combination of plasma explosion, optical breakdown and melting results in glass being well separated without cracking into multiple pieces.

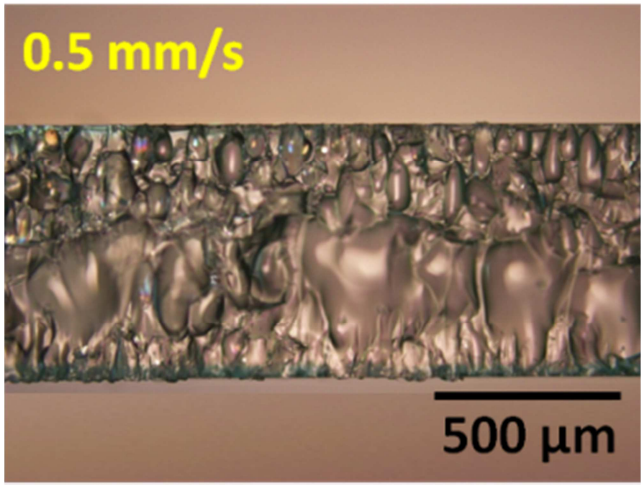

Figure 11. *Optical image of the sidewall of the glass cut at speed of 0.5 mm/s.*

At scanning speeds from 1 mm/s to 10 mm/s scanning speed, the laser energy deposition rate reduced from 8.96×104 μw/μm3 to 8.96×103 μw/μm^3 which led to top and bottom surfaces ablation with melting inside the glass as observed in figure 12. Due to the high deposition rate, many pulses were deposited which resulted in top and bottom surfaces ablation which could increase laser energy absorption and generate defects which lower the ablation threshold as discussed earlier for 0.5 mm/s scanning speed. Within this range of laser deposition rates, plasma explosion could not occur inside the glass as the laser deposition rate was not high enough to heat the plasma to higher temperatures required to drive plasma explosion as compared to 0.5 mm/s. Instead, the plasma was only heated up to sufficient temperatures to cause melting inside the glass. The extent of laser ablation at the glass top and bottom surfaces and melting inside the glass decreased as scanning speed increased. This could be due to decrease in laser deposition rate as an increase in scanning speed resulted in lesser pulses deposited into the glass.

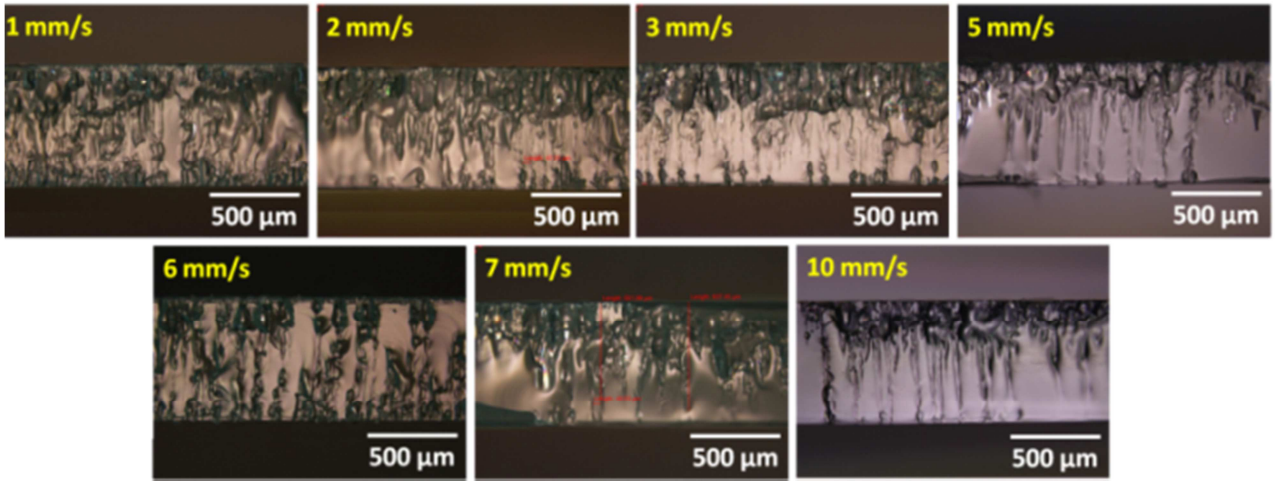

Figure 12. *Optical images of the sidewall of the glass cut at varied laser scanning speed from 1 mm/s to 10 mm/s.*

As laser scanning speed increased from 20 mm/s to 50 mm/s as shown in figure 10, the laser energy deposition rate decreased from 4.48×103 µw/µm^3 to 1.79×10^3 µw/µm^3 which resulted in cracks generated near the center of the glass thickness and voids at the bottom half of the glass thickness as shown in figure 13. Due to the lowered laser deposition rate, the plasma generated inside the glass was not heated high enough temperature to cause melting. Instead, thermal energy relaxation of plasma to lattice resulted in internal cracks formed near the center of the glass thickness. In addition, voids, slanting towards the direction opposite the direction of laser scanning, were observed at the bottom half of the glass thickness. This indicates that the remaining pulse energy after generating cracks at the center of the glass thickness is still sufficient to generate voids near the glass bottom surface by optical breakdown. The higher laser deposition rate of 4.48×103 µw/µm^3 at 20 mm/s scanning speed resulted in more cracks inside the glass. Thus, lesser laser energy was available to generate voids near the glass bottom surface by optical breakdown. As scanning speed increased to 30 mm/s, the deposition rate decreased to 2.99×103 µw/µm^3, which results in lesser cracks generated at the center of the glass. Thus, more pulse energy could be deposited at the laser focus to cause more voids by optical breakdown. As scanning speed was further increased to 50 mm/s, the laser deposition rate was further reduced to 1.79×103 µw/µm^3 led to lesser voids observed. This implies that the number of pulses deposited in a single spot played a major role in optical breakdown which in this case was independent of the laser intensity. In this case, the dominant free electron generation leading to optical breakdown could be due to thermal ionization instead of multi-photon ionization. The lower laser energy deposition rate by lesser pulses could be insufficient to cause thermal ionization of the atoms to form a plasma density above a critical value for optical breakdown to occur. This led to lesser voids observed at 50 mm/s.

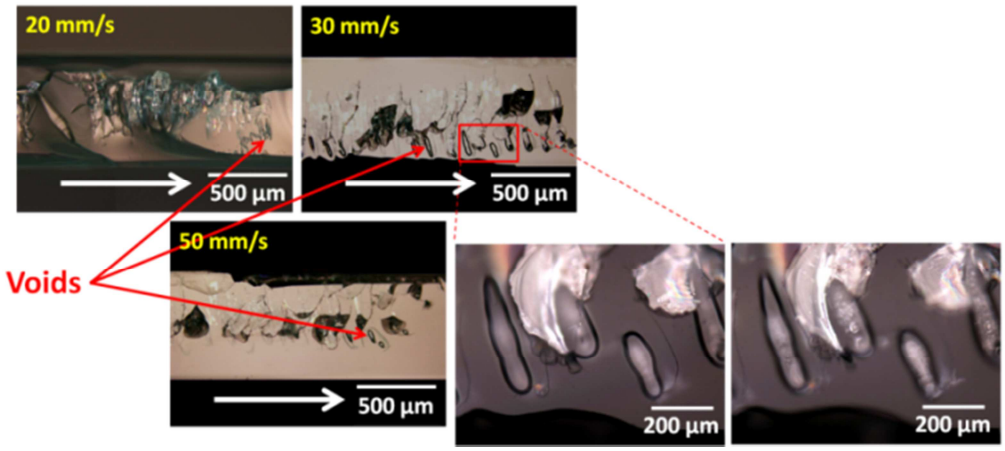

Figure 13. *Optical images of the sidewall of the glass cut at laser scanning speed from 20 mm/s to 50 mm/s.*

For 100 mm/s to 400 mm/s, the laser deposition rate reduced from 8.96×102 µw/µm^3 to 2.24×102 µw/µm^3. This resulted in mainly cracks formed inside the glass due to the lowered deposition rate as shown in figure 14. No optical breakdown occurred inside the glass. As Sun et al revealed that the reduced laser deposition rate could be insufficient to deposit enough pulses for thermal ionization of the atoms to occur for generating a critical plasma density for optical breakdown to happen [16].

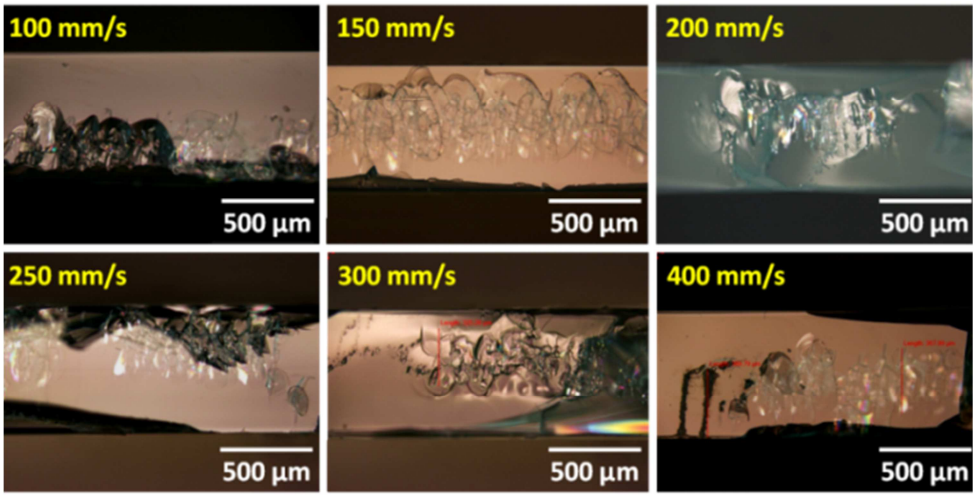

Figure 14. *Optical images of the sidewall of the glass cut at laser scanning speed from 100 mm/s to 400 mm/s.*

For 500 mm/s and 600 mm/s, the laser deposition rate was decreased to 1.79×102 µw/µm^3 and 1.49×102 µw/µm^3 respectively resulting in the void formation occurring near the glass top surface with melting tracks extending from the bottom of the void as shown in figure 15. The void formation only occurred in regions where crack deviation occurred from the cutting line. The void formation and melted tracks could be due to the refraction of the laser beam due to the crack deviation. The refracted beam could interfere with the original laser beam to form voids structures near the glass top surface as well the melted regions in the glass thickness. When the speeds were increased above 700 mm/s, nothing was noticeable inside the glass.

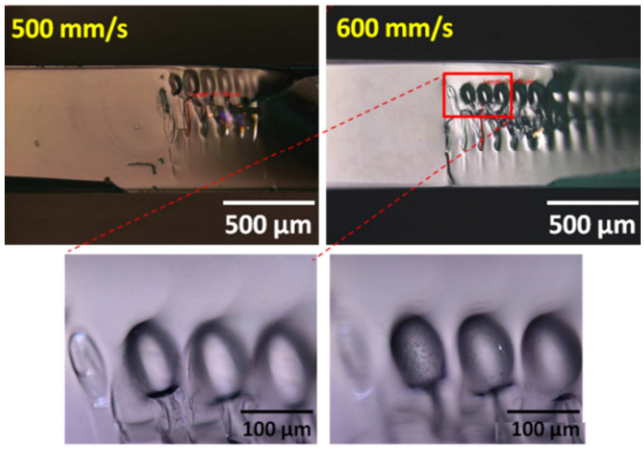

Figure 15. *Optical images of the sidewall of the glass cut at laser scanning speed from 500 mm/s to 600 mm/s.*

4. Conclusion

The study shows that ion exchanged Gorilla Glass could be effectively cut with picosecond near-infrared laser pulses for varied electronic applications. The results revealed that focus position is an important parameter in determining whether the glass can be well separated. At cutting speeds from 0.5 mm/s to 6 mm/s, when the laser focus was placed at 500 µm below the top surface for a 700 µm thick glass, namely more than half of the glass thickness, the glass could be well-separated into two pieces by non-linear absorption induced optical breakdown, melting, plasma explosion inside the glass. When the laser focus was placed near the top surface, V-shaped ablation grooves were generated at the glass top surface without glass separation. When the laser focus was placed inside the glass and near to the glass bottom surface, internal scribing occurred at the bottom part of the glass. The glass could also be separated by scribing-caused cracking throughout the glass entire thickness.

At the optimal focus ranges with speed of 0.5-6 mm/s, the optimal pulse frequency for well-cutting of the glass was found to be at a frequency of around 200 KHz, namely a proper laser fluence of 0.87 J/cm2 at the glass top surface. Low pulse frequencies of 50 KHz and 100 KHz produced higher laser fluences and 2.75 J/cm2 and 1.59 J/cm^2 respectively at the glass top surface. Glass top surface was ablated without glass separation. At high pulse frequencies of 300 KHz to 1000 KHz, the laser modified region leads the broken of the glass.

Under the optimal focuses and pulse frequency, the glass could be well-cut through without cracking into multiple pieces at scanning speeds from 0.5 mm/s to 6mm/s. The scanning speed together with pulse frequency determines the amount of laser pulse energy deposited into the glass. The time dependent energy amount could be described using laser energy deposition rate. The optimal laser deposition rate for cutting through the glass without breakage at 200 KHz pulse frequency was found to be between 1.54×105 µw/µm^3 at 0.5 mm/s to 1.29×104 µw/µm^3 at 6 mm/s. When the cutting speed was increased to more than 6 mm/s, the energy deposition rate was decreased and was below the required value for glass separation. The glass was cracked at the high speeds.

Acknowledgements

The study was performed under the project No. J13-M-13S funded by EPTL of Singapore and project No. C13-M-019 supported by A*Star Research Agency Singapore Institute of Manufacturing technology.

References

[1] Udrea M. 2000. Small power pulsed and continuous longitudinal CO2 Laser for material processing Proc. SPIE 4068 657-662

[2] Yamamoto K. Hasaka N. Morita H. Ohmura E. 2010. Influence of thermal expansion coefficient in laser scribing of glass Precision Engineering 34 70-75

[3] Hermanns C. 2000. Laser cutting of glass Proc. of SPIE 4102 219-226

[4] Du K. Shi P. 2003. Subsurface precision machining of glass substrates by innovative lasers Glass Sci. Technology 76 95-98

[5] Nikumba S. Chena Q. Lia C. Reshefa H. Zheng H. Y. Qiu H. Low D. 2005. Precision glass machining drilling and profile cutting by short pulse lasers Thin Solid Films 477 216– 221

[6] Abramov A. A. Black M. L. Glaesemann G. S. 2010. Laser separation of chemically strengthened glass Physics Procedia 5 285-290

[7] Russ S. Siebert C. Eppelt U. Hartmann C. Faißt B. Schulz W. 2013. Picosecond laser ablation of transparent materials Proc. of SPIE 8608 86080E-1-11

[8] Kumkara M. Bauerb L. Russb S. Wendela M. Kleinera J. Grossmanna D. Bergnerc K. Noltec S. 2014. Comparison of different processes for separation of glass and crystals using ultra short pulsed lasers Proc. of SPIE Vol. 8972 897214-1-16

[9] Haupt O. Müller D. Gäbler F. 2013. Shorter Pulse Widths Improve Micromachining EuroPhotonics 18 28-30

[10] Butkus S. Paipulas D. Sirutkaitis R. Sirutkaitis V. 2014. Rapid cutting and drilling of transparent materials via femtosecond laser filamentation Journal of Laser Micro/Nanoengineering 9 213-220

[11] Rekow M. Zhou Y. Falletto N. 2014. Precision glass processing with picosecond laser pulses Industrial Laser Solutions Mar/Apr. 11-14

[12] Wang Z. K. Zheng H. Y. Seow W. L. Wang X. C. 2015 Investigation on material removal efficiency in debris-free laser ablation of brittle substrates Journal of Materials Processing Technology 219 133-142

[13] Watanabe W. Tamaki T. Ozeki Y. Itoh K. 2010. Filamentation in Ultrafast Laser Material Processing in book "Progress in Ultrafast Intense Laser Science VI" Editors: Yamanouchi K. Gerber. G. Bandrauk A. D. Vol. 99 of the series Springer Series in Chemical Physics pp161-181

[14] Miyamoto I. Cvecek K. Schmidt M. 2011. Evaluation of nonlinear absorptivity in internal modification of bulk glass by ultrashort laser pulses Opt. Express 19 10714-10727

[15] Koubassov V. Laprise J. F. Théberge F. Förster E. Sauerbrey R. Müller B. Glatzel U. Chin S. L. 2004. Ultrafast laser-induced melting of glass Applied Physics A 79 499-505

[16] Sun M. Urs Eppelt Schulz W. Zhu J. 2013. Role of thermal ionization in internal modification of bulk borosilicate glass with picosecond laser pulses at high repetition rates Optical Materials Express 3 1716-1726

[17] Kaschke M. Donnerhacke K. H. Rill M. S. 2013. Optical Devices in Ophthalmology and Optometry: Technology Design Principles and Clinical Applications John Wiley & Sons Germany pp375-392

[18] Chin S. L. 2010. Femtosecond Laser Filamentation Springer Series On Atomic Optical And Plasma Physics pp. 6-8

[19] Karlsson S. Jonson B. Stålhandske C. 2010. The technology of chemical glass strengthening- a review European Journal of Glass Science and Technology A 51 41-54

[20] Steen W. Watkins K. G. Mazumder J. Laser Material Processing 2010 4thed Springer Science & Business Media London p. 91

[21] Machado L. M. Samad R. E. Rossi W. Junior N. D. V. 2012. D-Scan measurement of ablation threshold incubation effects for ultrashort laser pulses Optics Express 20 4114-4123

[22] Eaton S. M. Cerullo G. Osellame R. 2012. Fundamentals of Femtosecond Laser Modification of Bulk Dielectrics Femtosecond Laser Micromachining vol. 123 2012 complied by Roberto Osellame Giulio Cerullo Roberta Ramponi Topics in Applied Physics London pp 3-1